Research Article | Vol. 10, No. 7 | 1 Jul 2019 | BIOMEDICAL OPTICS EXPRESS 3584
Biomedical Optics EXPRESS

In vivo terahertz imaging to evaluate scar treatment strategies: silicone gel sheeting

JIARUI WANG,[1] QIUSHUO SUN,[1] RAYKO I. STANTCHEV,[1] TOR-WO CHIU,[2] ANIL T. AHUJA,[3] AND EMMA PICKWELL-MACPHERSON[1,4,*]

[1]*Department of Electronic Engineering, The Chinese University of Hong Kong, Shatin, Hong Kong, China*
[2]*Division of Plastic Reconstructive and Aesthetic Surgery, Department of Surgery, The Chinese University of Hong Kong, Shatin, Hong Kong, China*
[3]*Department of Imaging and Interventional Radiology, Chinese University of Hong Kong, Hong Kong, China*
[4]*Department of Physics, University of Warwick, Coventry, United Kingdom*
**e.pickwell.97@cantab.net*

Abstract: Silicone gel sheeting (SGS) is widely used for scar treatment; however, studies showing its interaction with skin and efficacy of scar treatment are still lacking. THz light is non-ionizing and highly sensitive to changes in water content and thus skin hydration. In this work, we use *in-vivo* THz imaging to monitor how SGS affects the THz response of human skin during occlusion, and the associated THz reflectivity and refractive index changes are presented. We find that SGS effectively hydrates the skin beneath it, with minimal lateral effects beyond the sheeting. Our work demonstrates that THz imaging is able to detect the subtle hydration changes on the surface of human skin caused by SGS, and it has the potential to be used to evaluate different scar treatment strategies.

1. Introduction

Hypertrophic and keloid scars frequently occur on human skin after surgery and burn injuries [1,2]. Current treatment methods include but are not limited to applying tretinoin cream, pulsed dye laser therapy and surgical excision. Silicone gel, in either sheet or an ointment form, is widely used in clinical treatment for healing and preventing hypertrophic and keloid scars because of the ease of application, high efficiency and minimal side effects [1,3,4]. However, the mechanism of action is unclear [1]. The semi-occlusive nature of silicone gel sheeting (SGS) provides hydration that causes a decrease in trans-epidermal water loss (TEWL). It also normalizes the hydration state of keratinocytes and signals to dermal fibroblasts to downregulate the production of collagens [3,5]. Additionally, the temperature and static electric field changes upon applying SGS might also play a role in the treatment [2,6,7]. It is therefore important to quantitatively monitor the SGS treatment *in vivo* and understand the mechanisms and effects of SGS. However, current assessment techniques of scar healing, use scar shape, colour, texture and thickness, but they are subjective and external [8,9]. Therefore, a quantitative technique which can also determine the internal characteristics and functionality of skin is needed.

Terahertz (THz) light, typically defined as 0.1 THz~10 THz, is non-invasive and highly sensitive to water, making it a favorable tool for *in vivo* skin characterization [10]. THz time domain spectroscopy has the potential to assess water concentration in tissues both *ex vivo* and *in vivo* [11,12]. However, the high absorption by water constrains THz *in vivo* measurements to a reflection geometry and an imaging window is usually employed for accurate positioning [13,14]. Fan et al. used THz reflection imaging to observe the scar recovery process for six months and found that THz imaging could reveal a scar that was almost invisible to the naked eye, indicating the potential of THz imaging to aid scar

#364297 https://doi.org/10.1364/BOE.10.003584
Journal © 2019 Received 5 Apr 2019; revised 18 May 2019; accepted 27 May 2019; published 25 Jun 2019

Biomedical Optics EXPRESS

treatment and management [15]. Hernandez-Cardoso *et al*. showed that THz imaging could be used to detect early stages of microvascular damage in the diabetic foot based on different skin hydration levels [16]. During *in vivo* THz measurements, there are several variables including contact pressure and skin occlusion that can affect the skin properties and THz results; these factors need to be accounted for to achieve accurate characterization [17]. During *in vivo* measurements, the pressure between the imaging window and the skin area of interest affects the THz signal as the skin becomes compressed at higher pressures [17]. Additionally, contacting the imaging window blocks the pores on the skin, causing occlusion [18]. The reflected THz signal is very sensitive to the changes in hydration caused by occlusion. Thus, in this study, we carefully control the contact pressure and duration in addition to usual THz system settings to demonstrate how THz imaging can be used to evaluate the effectiveness of SGS treatment.

2. Method

2.1 Experimental setup and protocols

The study was approved by the Joint CUHK-NTEC Clinical Research Ethics Committee: informed, signed consent was obtained from all volunteers who participated. A THz time-domain reflection system (Menlo K15) was used for the THz measurements. As indicated in Fig. 1(a), subjects placed their arm on a quartz window to be in the focus of the THz beam, and the reflected signal from the skin was then measured. The THz emitter and detector could also be scanned to obtain an image without moving the sample. Two types of THz measurements were taken in the study: point scan and imaging scan measurements. For point scans, the THz beam was focused onto a single point on the skin and measured at an acquisition frequency of 4 Hz. In the imaging mode the THz beam was moved in only the y direction to image one line with 0.5 mm per step. Aluminum foil with different apertures cut (30 × 20mm for point scan, 20 × 40mm for line scan) was put on the imaging window and the skin marked with pen at the corners (as illustrated in Figs. 1(b) and 1(c)) to ensure that the same location was measured during each measurement. Also as part of the experimental protocol, to control any temperature variation, volunteers were required to be in the temperature controlled laboratory for 20 minutes prior to each measurement. No significant temperature changes were found in the 10 subjects before and after applying silicone gel or the SGS.

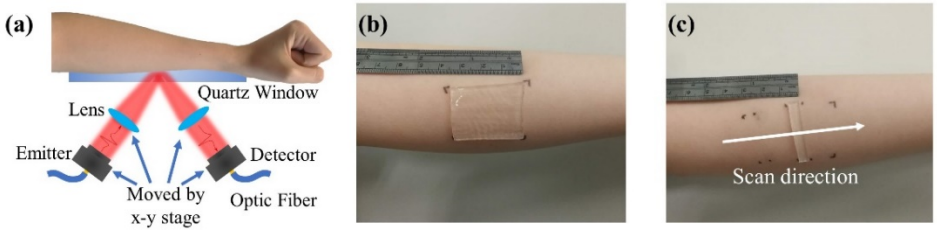

Fig. 1. (a) Experiment setup. Photograph of the (b) SGS (c) a slim strip of SGS.

Point scan measurements. The normal state of skin was measured continuously for 1 minute (240 waveforms) then after at least one-hour rest, each subject was asked to apply a piece of 30 × 20mm SGS (Self-adhesive CICA-CARE) on the marked area for 4 hours, as illustrated in Fig. 1(b). After the treatment, the same area was re-measured for 60 s. The contact pressure between the skin and the quartz window was recorded: subjects had real-time feedback to help them control it to be between 2.0 and 2.5 N/cm^2. Note that to optimize control of the variables, subjects were asked to quickly remove the SGS and place the target area on the imaging window for immediate measurement. To compare the effects of silicone gel with SGS, we also conducted a point scan measurement with silicone gel (BAPSCARCARE gel with UV protection) applied to the area of interest.

Biomedical Optics EXPRESS

Line scan measurements. For the line-imaging scan, a 5 mm × 20 mm strip of SGS was applied to the volar forearm for 4 hours and after removing the SGS, a line scan was taken with the scan direction perpendicular to where the strip had been, as indicated in Fig. 1(c). For further comparison, a 5 mm × 20 mm strip of wet bandage (which had been soaked in water for 5 minutes and then wrung out), was also applied to skin.

2.2 Data processing

When measuring samples placed on a quartz window in reflection geometry, there are two reflections that need to be considered, one from the air-quartz interface and one from quartz-sample interface. An empty quartz window i.e. air was measured for the reference. The first reflection is defined as the baseline – this was measured by placing another identical piece of quartz on the imaging window with a drop of ethanol between them (for better contact) to eliminate the second reflection. The separation of the baseline from the sample reflection is dependent on the quartz thickness: we used our group's previous algorithm to eliminate the thickness variation of the quartz window [19]. The equations to determine the processed signal and reflectivity(R) are also fully detailed in [17,19]. In short, the frequency domain result is calculated from the time domain signal by Fourier Transform. The signal is then filtered by a double Gaussian filter with 0.1 THz and 0.6 THz as cut-off frequencies to get the processed signal. Human skin can be considered as a multilayered structure comprising the stratum corneum (SC), epidermis and dermis [20,21]. Here we model skin as a two layer structure with each layer consisting of water and biological background [12,16]. The SC and epidermis water percentages vary before and after applying SGS as does the SC thickness. By using effective medium theory (Landau,Lifshitz, Looyenga (LLL) model), we calculated the permittivity of each layer [11] and deduced the reflection coefficient of a three layer quartz-SC-epidermis structure (Eq. (1)):

$$r_{\mathrm{qse}} = \frac{r_{qs} + r_{se}\exp(-i2\beta)}{1 + r_{qs}r_{se}\exp(-i2\beta)} \tag{1}$$

$$M_{cal} = \frac{r_{qse}}{r_{qa}} = M_{meas} \tag{2}$$

where r_{qs}, r_{se} are the reflection coefficients of the quartz-SC and SC-epidermis interfaces calculated from Fresnel Equations [17]. The phase variation β is given by $\beta = 2\pi d_{sc}N_{sc}\cos\theta_{sc}/\lambda$, where N_{sc}, d_{sc}, θ_{sc} and λ are the complex refractive index, thickness and incident angle of the SC and wavelength of incident light. By dividing the reflection coefficient of the three layer model (r_{qse}) with the reflection coefficient of quartz-air(r_{qa}) [17], the reflection ratio, M_{cal}, is obtained (Eq. (2)) and is a function of several parameters including the SC and epidermis water concentration and SC thickness. We therefore fit the calculated reflection ratio to our measured sample-air ratio to deduce the unknown parameters. These values can then be combined with effective medium theory to calculate the refractive index of the SC and epidermis before and after applying SGS.

3. Results and discussion

3.1 THz response of skin before and after treatment

Figures 2(a)–2(d) display the THz properties of skin before and after applying SGS for up to 4 hours. Figure 2(a) shows how the time domain processed signal reduces in amplitude as the time of wearing the SGS increases. Before applying the sheeting (blue data, Fig. 2(b)) the peak-to-peak response decreases with time during the 60s measurement, as the quartz window is occluding the skin and causing water to accumulate in the SC. Time t = 0 is defined as the time at which the skin made contact with the quartz window. We measured the THz response

Biomedical Optics EXPRESS

for wearing the sheeting for up to 12 hours, but the greatest changes were in the first 4 hours. After 4 hours of wearing the silicone sheeting, the SC is almost saturated already, so there is minimal further change in the skin when occluded by the window and thus the red line in Fig. 2(b) is fairly flat. Changes in the optical properties of the skin affect its reflectivity which in turn affects the measured time domain signals. The reflectivity is plotted in Fig. 2(c); since this depends on the refractive indices of the quartz and the skin, it is significantly frequency dependent. After 4 hours of occlusion by the SGS, the peak to peak of the processed signal significantly decreased (Fig. 2(b)). In contrast, as illustrated in Fig. 2(d), the silicone gel caused almost no change to the THz signal, suggesting the product is less effective at occluding the skin. Thus, we focus our study on the SGS.

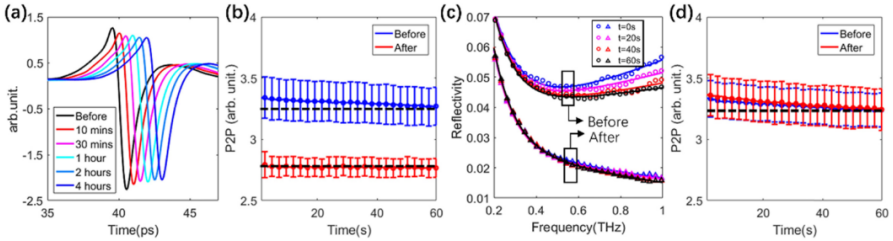

Fig. 2. (a) Processed signal before and after 10 mins, 30 mins, 1hr, 2 hrs and 4 hrs of SGS application; (b) Averaged peak to peak of the processed signal before and 4 hrs after SGS application; (c) Reflectivity after 0, 20, 40 and 60 s of occlusion for before and after 4hrs of SGS application; and (d)Averaged peak to peak of the processed signal before and 4 hrs after applying silicone gel. The dashed black lines in (b) and (d) are horizontal visual guides. Error bars are the standard deviations from averaging over 10 subjects.

From the 2-layer model (detailed in section 2.2) we found that the average water concentration of the epidermis for the 10 subjects did not change significantly and was 75.7 ± 2.9% and 76.9 ± 2.5% before and after SGS application. However, significant changes were observed in the SC hydration and we also found that the SC thickness increased. Figure 3(a) shows that the calculated average water percentage in the SC after 4 hrs of SGS application was significantly higher than before application. As illustrated in Fig. 3(b) the refractive index of the SC increased due to the SGS application but the refractive index of the epidermis was not significantly affected as it maintained almost constant hydration. It should be noted that the discrepancy between the extracted refractive index in this work and that in reference [17] is due to the different models employed. Here we model the skin by considering the SC and epidermis as 2 homogenous layers whereas in reference [17] we treated skin as a single layer when calculating refractive index. In Fig. 3(c) we plot a colour-map for one subject to highlight how, due to applying the SGS, the water concentration in the SC (at t = 0) increased from 24% to 58% and the SC thickness increased with increasing water concentration.

3.2 Lateral extent of hydration and recovery of the skin

In this section we use the THz line scan image data to see contrast between skin where the SGS was applied and nearby skin. In this way, we can quantify the effects caused by the SGS and determine the lateral extent for different time points.

Biomedical Optics EXPRESS

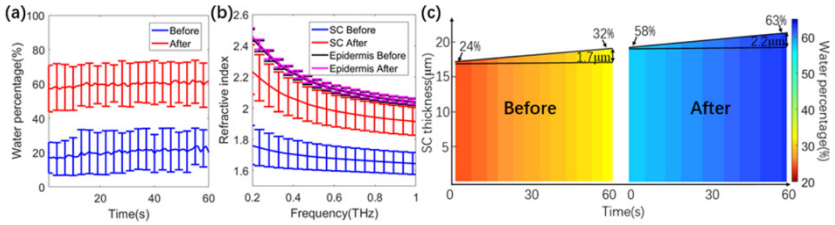

Fig. 3. (a)Averaged water concentration in SC during a 60 s measurement before and after applying SGS for 4 hours; (b) Averaged refractive index at t = 30s. Error bars are the standard deviations from averaging over 10 subjects; (c) Colour-map of the SC hydration and thickness during a 60s measurement before and after applying SGS.

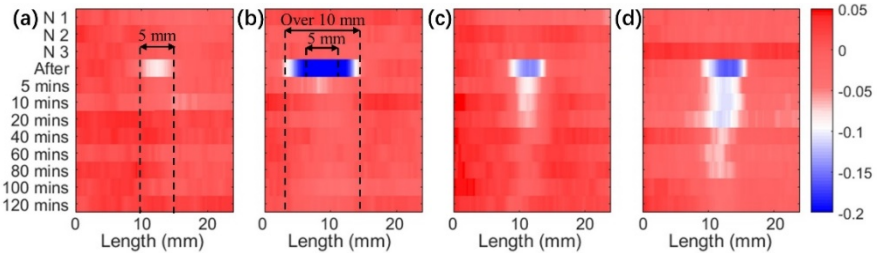

Fig. 4. Peak to peak images from line scan measurements after skin was occluded by (a) SGS and (b) a wet bandage for 10 minutes. Recovery of the skin after the SGS was removed having been applied for (c) 4 hours and (d) 12 hours.

The N1, N2, and N3 measurements in Fig. 4 are three repeated line scan measurements of the skin before application of the SGS or wet bandage. The plotted peak to peak of the processed signal is normalized by the averaged amplitude of the normal skin prior to application of the SGS or wet bandage. Each line represents a line scan measurement at a different time (indicated on the left). As shown in Fig. 4(a), the peak to peak of the processed signal remained decreased slightly after 10 minutes of applying the 5 mm strip of SGS: the decrease in the normalized peak to peak corresponds to increased hydration. The effect is confined to the skin that was directly below the 5 mm strip. In contrast, when the 5 mm strip of wet bandage was applied, the skin beneath it and also extending across a 10 mm width was also affected (Fig. 4(b)) and hydrated to a greater extent. This increase in hydration could only be detected at the 5 minutes post-removal measurement. Applying the SGS for longer increased the skin hydration, but it was almost saturated after 4 hours suggesting that the recovery of the skin depends on the duration that the sheeting was worn for. Figure 3(c) shows that some increase in hydration can still be detected for 20 minutes after removal if only worn for 4 hours, and after 80 minutes if worn for 12 hours (Fig. 4(d)). Thus, for maximum hydration increase, it is better to wear the sheeting as continuously as possible. These results indicate that the SGS only occludes the skin and increases the hydration level in the applied area, in other words the water does not diffuse to the surrounding area. However, for the wet bandage the beneficial effects will be short-lived and water will also diffuse to surrounding areas, significantly increasing the water content nearby.

4. Conclusion

In this work, we have demonstrated how THz spectroscopy and imaging can be used to monitor the effects of SGS. Our results show that SGS has an occlusive effect on skin and increases the hydration of the skin that is directly beneath the sheeting only, and that SGS is more effective at increasing the skin hydration than silicone gel. However, after removing SGS, the skin will recover back to its normal state within 80 minutes, depending on how long the sheeting was applied for. This may be useful information for clinical treatment. More importantly, this study has illustrated how THz imaging can quantitatively measure changes

Biomedical Optics EXPRESS

in water concentration in skin. This could be very useful to dermatologists as well as the cosmetic community for optimizing skin treatment strategies and product development.

Funding

Research Grants Council of Hong Kong (14206717 and 14201415), The Hong Kong Innovation and Technology Fund (ITS/371/16), the Hong Kong PhD Fellowship Award, and the Royal Society Wolfson Merit Award.

Disclosures

The authors declare that there are no conflicts of interest related to this article.

References

1. D. Stavrou, O. Weissman, E. Winkler, L. Yankelson, E. Millet, O. P. Mushin, A. Liran, and J. Haik, "Silicone-based scar therapy: a review of the literature," Aesthetic Plast. Surg. **34**(5), 646–651 (2010).
2. B. Berman, O. A. Perez, S. Konda, B. E. Kohut, M. H. Viera, S. Delgado, D. Zell, and Q. Li, "A review of the biologic effects, clinical efficacy, and safety of silicone elastomer sheeting for hypertrophic and keloid scar treatment and management," Dermatol. Surg. **33**(11), 1291–1303 (2007).
3. T. A. Mustoe, "Evolution of silicone therapy and mechanism of action in scar management," Aesthetic Plast. Surg. **32**(1), 82–92 (2008).
4. S. Y. Kwon, S. D. Park, and K. Park, "Comparative effect of topical silicone gel and topical tretinoin cream for the prevention of hypertrophic scar and keloid formation and the improvement of scars," J. Eur. Acad. Dermatol. Venereol. **28**(8), 1025–1033 (2014).
5. T. A. Mustoe and A. Gurjala, "The role of the epidermis and the mechanism of action of occlusive dressings in scarring," Wound Repair Regen. **19**(Suppl 1), s16–s21 (2011).
6. M. A. Musgrave, N. Umraw, J. S. Fish, M. Gomez, and R. C. Cartotto, "The effect of silicone gel sheets on perfusion of hypertrophic burn scars," J. Burn Care Rehabil. **23**(3), 208–214 (2002).
7. B. Hirshowitz, E. Lindenbaum, Y. Har-Shai, L. Feitelberg, M. Tendler, and D. Katz, "Static-electric field induction by a silicone cushion for the treatment of hypertrophic and keloid scars," Plast. Reconstr. Surg. **101**(5), 1173–1183 (1998).
8. P. S. Powers, S. Sarkar, D. B. Goldgof, C. W. Cruse, and L. V. Tsap, "Scar assessment: current problems and future solutions," J. Burn Care Rehabil. **20**(1 Pt 1), 53–60 (1999).
9. P. P. M. van Zuijlen, A. P. Angeles, R. W. Kreis, K. E. Bos, and E. Middelkoop, "Scar assessment tools: implications for current research," Plast. Reconstr. Surg. **109**(3), 1108–1122 (2002).
10. Q. Sun, Y. He, K. Liu, S. Fan, E. P. J. Parrott, and E. Pickwell-MacPherson, "Recent advances in terahertz technology for biomedical applications," Quant. Imaging Med. Surg. **7**(3), 345–355 (2017).
11. Y. He, K. Liu, C. Au, Q. Sun, E. P. J. Parrott, and E. PickWell-MacPherson, "Determination of terahertz permittivity of dehydrated biological samples," Phys. Med. Biol. **62**(23), 8882–8893 (2017).
12. D. B. Bennett, W. Li, Z. D. Taylor, W. S. Grundfest, and E. R. Brown, "Stratified media model for Terahertz reflectometry of the skin," IEEE Sens. J. **11**(5), 1253–1262 (2011).
13. N. Bajwa, J. Au, R. Jarrahy, S. Sung, M. C. Fishbein, D. Riopelle, D. B. Ennis, T. Aghaloo, M. A. St John, W. S. Grundfest, and Z. D. Taylor, "Non-invasive terahertz imaging of tissue water content for flap viability assessment," Biomed. Opt. Express **8**(1), 460–474 (2016).
14. R. M. Woodward, B. E. Cole, V. P. Wallace, R. J. Pye, D. D. Arnone, E. H. Linfield, and M. Pepper, "Terahertz pulse imaging in reflection geometry of human skin cancer and skin tissue," Phys. Med. Biol. **47**(21), 3853–3863 (2002).
15. S. Fan, B. S. Y. Ung, E. P. J. Parrott, V. P. Wallace, and E. Pickwell-MacPherson, "In vivo terahertz reflection imaging of human scars during and after the healing process," J. Biophotonics **10**(9), 1143–1151 (2017).
16. G. G. Hernandez-Cardoso, S. C. Rojas-Landeros, M. Alfaro-Gomez, A. I. Hernandez-Serrano, I. Salas-Gutierrez, E. Lemus-Bedolla, A. R. Castillo-Guzman, H. L. Lopez-Lemus, and E. Castro-Camus, "Terahertz imaging for early screening of diabetic foot syndrome: A proof of concept," Sci. Rep. **7**(1), 42124 (2017).
17. J. Wang, R. I. Stantchev, Q. Sun, T.-W. Chiu, A. T. Ahuja, and E. P. MacPherson, "THz *in vivo* measurements: the effects of pressure on skin reflectivity," Biomed. Opt. Express **9**(12), 6467–6476 (2018).
18. Q. Sun, R. I. Stantchev, J. Wang, E. P. J. Parrott, A. Cottenden, T.-W. Chiu, A. T. Ahuja, and E. Pickwell-MacPherson, "In vivo estimation of water diffusivity in occluded human skin using terahertz reflection spectroscopy," J. Biophotonics **12**(2), e201800145 (2019).
19. X. Chen, E. P. J. Parrott, B. S. Y. Ung, and E. Pickwell-Macpherson, "A Robust Baseline and Reference Modification and Acquisition Algorithm for Accurate THz Imaging," IEEE Trans. Terahertz Sci. Technol. **7**(5), 493–501 (2017).
20. M. Ney and I. Abdulhalim, "Modeling of reflectometric and ellipsometric spectra from the skin in the terahertz and submillimeter waves region," J. Biomed. Opt. **16**(6), 067006 (2011).

Biomedical Optics EXPRESS

21. Y. Feldman, A. Puzenko, P. Ben Ishai, A. Caduff, I. Davidovich, F. Sakran, and A. J. Agranat, "The electromagnetic response of human skin in the millimetre and submillimetre wave range," Phys. Med. Biol. **54**(11), 3341–3363 (2009).